Published in final edited form as:
*Bioorg Med Chem*. 2022 July 01; 65: 116785. doi:10.1016/j.bmc.2022.116785.

# Short peptide pharmacophores developed from protein phosphatase-1 disrupting peptides (PDPs)

**Miriam Fontanillo**[a], **Malgorzata Trebacz**[b,c], **Christopher D. Reinkemeier**[a], **Daniela Avilés Huerta**[a], **Ulrike Uhrig**[d], **Peter Sehr**[d], **Maja Köhn**[a,b,c,*]

[a]Genome Biology Unit, EMBL, Heidelberg, Germany

[b]Centres for Biological Signalling Studies BIOSS and CIBSS, University of Freiburg, Freiburg, Germany

[c]Faculty of Biology, University of Freiburg, Schänzlestrasse 18, 79104 Freiburg, Germany

[d]Chemical Biology Core Facility, EMBL, Heidelberg, Germany

## Abstract

PP1 is a major phosphoserine/threonine-specific phosphatase that is involved in diseases such as heart insufficiency and diabetes. PP1-disrupting peptides (PDPs) are selective modulators of PP1 activity that release its catalytic subunit, which then dephosphorylates nearby substrates. Recently, PDPs enabled the creation of phosphatase-recruiting chimeras, which are bifunctional molecules that guide PP1 to a kinase to dephosphorylate and inactivate it. However, PDPs are 23mer peptides, which is not optimal for their use in therapy due to potential stability and immunogenicity issues. Therefore, we present here the sequence optimization of the 23mer PDP to a 5mer peptide, involving several attempts considering structure-based virtual screening, high throughput screening and peptide sequence optimization. We provide here a strong pharmacophore as lead structure to enable PP1 targeting in therapy or its use in phosphatase-recruiting chimeras in the future.

### Keywords

Protein phosphatase-1; PP1-disrupting peptides; Peptide pharmacophore; High throughput screening; Virtual screening; Rational peptide design; Structure–activity relationship study



*Corresponding author. maja.koehn@bioss.uni-freiburg.de (M. Köhn).

**Declaration of Competing Interest**

The authors declare that they have no known competing financial interests or personal relationships that could have appeared to influence the work reported in this paper.

*Author contributions*

M.F., C.D.R. and D.A.H. synthesized and tested all compounds *in vitro*. M.F., M.T. and D.A.H. tested compounds in calcium release assay, M.T. in H3pT3 assay. U.U. carried out the virtual screen, P.S. the HTS. M. F., U.U, P.S. and M.K. designed experimental strategies and wrote the manuscript. M.K. supervised the experiments, obtained funding and conceptualized the study.

## 1 Introduction

PP1 is a ubiquitously expressed protein serine/threonine phosphatase[1] and it is estimated to counteract over hundred kinases.[2–3] The activity, substrate specificity and localization of PP1 are regulated by the interaction with different, structurally unrelated regulatory interactors of protein phosphatase one (RIPPOs).[3–6] The catalytic subunit of PP1 presents several binding sites and most RIPPOs bind to the “RVxF” hydrophobic channel, named according to the most common amino acids present in RIPPOs that bind to this pocket. To date, PP1 is known to be involved in a wide range of cellular processes such as mitosis,[7] calcium signalling [8–10] and cardiovascular processes.[11–12] Accordingly, dysregu-lation or malfunction of these tightly regulated processes can lead to several diseases such as cancer, heart insufficiency or diabetes. In order to understand the pathways in which PP1 is involved and evaluate its therapeutic potential, an appealing approach consists of developing peptides that target the RVxF-binding site of PP1 and disrupt PP1-RIPPO interactions.[13]

Different peptides and peptidomimetics based on RIPPO sequences have been developed.[13–16] The 23mer PP1 disrupting peptides (PDPs), such as PDP3 (Ac-RRKRPKRKRKNA**RVTF**-*Bpa*-EAAEII-$NH_2$), were the first to be reported as active compounds both *in vitro* and in intact cells.[13] They disrupt PP1 holoenzymes to release the catalytic subunit, which can dephosphorylate nearby substrates (Fig. 1).[13] As an example for their application, PDP3 treatment was shown to seal the arrhythmogenic sarcoplasmic reticulum-$Ca^{2+}$-leak, which when untreated leads to heart failure. Thus, releasing PP1 activity may represent a promising future antiarrhythmic therapeutic approach.[12] However, while active in cell and tissue culture, 23mer peptides can pose challenges such as immunogenicity and insufficient stability in an organism. In addition, PDPs were used to create phosphatase-recruiting chimeras (PhoRCs, a similar principle is also named PhosTACs,[17]) in order to guide PP1 to dephosphorylate and inactivate an oncogenic kinase.[18] While these were somewhat active in intact cells, making a bifunctional molecule from a long peptide can also pose challenges for cell permeability.[18] Developing a small molecule or a shorter pharmacophore from the 23mer PDP would be the first step toward solving such challenges.

## 2 Materials and methods

### 2.1 Virtual screen

2.8 million compounds from the available screening catalogues of the commercial vendors Enamine and ChemBridge were downloaded and 3D coordinates were generated as input for the docking software SurflexDock v.2.51 from BioPharmics IT as implemented in the software package SYBYL-X 1.3, Tripos, 1699 South Hanley Rd., St. Louis, Missouri, 63144, USA. The crystal structure of PP1, deposited in the protein database (https://www.ebi.ac.uk/pdbe/) with the pdb-code 4G9J was downloaded and prepared. With the help of the protein preparation tool inside the software package the protein got analysed and completed. The region which interacts with the sequence RVTF of the co-crystallized peptide PDP2 (included in the used protein (4G9J)) was defined as the docking site. All prepared small molecules were flexibly docked into this region. As primary filter only the compounds which yielded a high docking score were selected (defined threshold >= 7.0).

Further the docked poses of the compounds were checked for fulfilling at least two of the four pharmacophoric features (two hydrophobic groups, a hydrogen bond donor and a hydrogen bond acceptor). These were identified to be important for binding after visual inspection of crystal structures of several PP1 with PIPs binding to the RVxF binding. Finally, the docked compounds were visually checked and 58 got prioritized and purchased for *in vitro* testing as described below.

### 2.2 High throughput screening (HTS) and dose-response testing of potential hit compounds

A high throughput screen of 79,000 compounds at 40 μM for modulators of the PP1 activity inhibited by I2 was performed at the Chemical Biology Core Facility at EMBL. Dephosphorylation of the fluorogenic substrate 6,8-difluoro-4-methylumbelliferylphosphate (DiFMUP) by PP1 was monitored by the increase in fluorescence at 460 nm after excitation at 340 nm in a kinetic mode to circumvent the interference of compounds showing auto-fluorescence.[19] With 40 pM PP1, 40 pM I2 and 20 μM of DiFMUP in 50 mM imidazole pH 7.5, 10 mM NaCl, 2 mM DTT, 1 mM $MnCl_2$, 0.05% Tween 20 and 0.1% BSA a sufficient linear increase in fluorescence over 3 h was achieved with around 80% inhibition of PP1 activity. These conditions made the assay suitable to find both PP1 inhibitors and compounds disrupting the interaction between PP1 and I2, leading to de-inhibition of PP1. Pre-plated compounds were incubated with PP1 for 15 min, then I2 was added and incubated for 15 min and finally, the substrate DiFMUP was added and fluorescence intensity measured in kinetic mode on an Envision plate reader (PerkinElmer). Time-series data were subject to linear regression analysis in Activity-Base software (IDBS). Finally, 58 compounds inducing over 40% of non-inhibited PP1 activity were selected from the HTS and purchased from the suppliers for conformation of their activity in the screening assay in dose-response from 200 μM to 200 nM and in parallel for specificity of their effect on PP1 phosphatase activity in a counter assay without PP1/ I2 in the reagent mix. PDP3 served as internal control standard on each assay plate. The 58 compounds from the virtual screen were tested in a similar way.

### 2.3 General materials and methods for the peptide synthesis and biochemical assays

Solvents were purchased and used as received from the following suppliers: *N,N*-dimethylformamide (DMF), acetic anhydride and dimethylsulfoxide (DMSO) from Merck; *N*-methyl-2-pyrrolidone (NMP), diethylether, piperidine and pyridine from ROTH; *N,N*-diisopropyle-thylamine (DIPEA) from abcr; acetonitrile (ACN) ≥ 99.9% HPLC grade, HPLC water LCMS chromasolv and methanol (MeOH) ≥ 99.9% HPLC grade from Sigma-Aldrich; deuterium oxide ($D_2O$) 99.95% and meth-anol-$d_4$ ($CD_3OD$) 99.8% from deutero GmbH.

Materials were used without further purification from the following commercial sources: Fmoc-Gly-OH, Fmoc-Leu-OH, Fmoc-Orn(Boc)–OH, Fmoc-Lys(Boc)-OH, Fmoc-Val-OH, Fmoc-His-OH, Fmoc-Phe-OH, Fmoc-β-homo-Lys-OH, Fmoc-homo-Arg(Pbf)–OH, Fmoc-Cpg-OH, Fmoc-*N*-Me-Phe-OH, Fmoc-D-Arg(Pbf)–OH, Fmoc-D-Lys-OH, H-D-Phe Wang resin, Rink amide resin, triethylamine (TEA), sodium chloride, glycerol and ethylenediaminetetraacetic acid (EDTA) from Merck Novabiochem; 2-(1H-ben-zotriazol-1-

yl)-1,1,3,3-tetramethyluronium hexafluorophosphate (HBTU), Fmoc-*N*-Me-Arg(Mtr)OH and H-Phe-2-chlorotrityl resin 200–400 mesh 0.5–0.9 mmol/g substitution from Bachem; Fmoc-Arg(Pbf)-OH from GL Biochem (Shanghai); Fmoc-L-β-homo-Phe-OH, Fmoc-L-β-Phe-OH and triisopropylsilane (TIPS) from Alfa Aesar; Fmoc-homo-Lys-OH, 7-diethylami-nocoumarin-3-carboxylic acid, Triton X-100, imidazole ≥ 99.5%, dithiothreitol (DTT) and manganese(II) chloride tetrahydrate ≥ 99% from Sigma-Aldrich; Fmoc-L-cyclopropylglycine from ChemImpexI; Fmoc-8-amino-3,6-dioxaoctanoic acid from PolyPeptid; Fmoc-β-homo-Arg(Pbf)-OH from Aapptec; Fmoc-D-His-OH from IrisBiotech; Fmoc-Pra-OH from aapptech; hydroxybenzotriazole (HOBT) from MOLEKULA; trifluoroacetic acid (TFA) from ROTH; 1-hydroxy-7-azabenzotriazole (HOAT) and *O*-7-Azabenzotriazol-1-yl-1,1,3,3-tetramethyluronium hexafluorophosphate (HATU) from GL Biochem (Shanghai) Ltd; Dulbecco's Modified Eagle's Medium (DMEM), DiFMUP and Fluo-4 from Life Technologies; and Fetal Bovine Serum (FBS) from Thermo Fisher Scientific. PP1 and I2 were prepared as previously described.[20]

Optical rotation was measured with Polatronic H532 polarimeter (Schmidt Haensch). $[\alpha]_D^{20}$ were reported in degmlg$^{-1}$dm$^{-1}$ and the concentration was in g/100 ml. $^1$H and $^{13}$C NMR spectra were recorded using Bruker UltraShield Avance III HD 400, 500 or 700 MHz using Topspin 3.2 as acquisition software and MestReNova 10.0 to analyze all data. Chemical shifts were quoted in ppm and reported using solvent as an internal standard: $^1$H NMR: 3.31 ppm (CD3OD), $^{13}$C NMR: 49.00 ppm (CD3OD). In NMR experiments using $D_2O$, $^1$H NMR peaks were referenced using the solvent as an internal standard (4.766 ppm) and chemical shifts adjusted according to the temperature.[21] $^{13}$C NMR peaks were referenced indirectly relative to the proton reference considering the known gyromagnetic ratio.[21] 2D COSY, HSQC, HMBC and ROESY spectra were used to assist NMR signal assignments. Automatic synthesis of compounds was performed with a MultiSynTech Syro I Parallel Peptide Synthesis System using 5 ml plastic reactors with TF frit (from Multisyntech). Manual synthesis of peptides on solid phase and cleavage from the resin was performed using 5 ml or 2 ml reactors with TF frit and plastic plunges (from Multisyntech). Analytical HPLC runs (1.5 ml/min) and purifications (5 ml/min) were performed on a Shimadzu HPLC-MS 2010EV Evolution system with a reversed phase column from Macherey-Nagel (NUCLEODUR 100-5C18ec 250/4.0 or NUCLEODUR C18pyramid VP250/4.6 3 μm particle size for analytical runs and NUCLEODUR C18pyramid VP250/10 5 μm particle size for purifications) with a UV/ Vis detector operating at λ = 215 and 254 nm. As mobile phases, ACN/ 0.05% TFA and $H_2O$/0.05% TFA were used.

### 2.4 Synthesis of compounds

Peptides were synthesized on solid support on a peptide synthesizer doing double couplings for 40 min using Fmoc-amino acids (5 equiv), HBTU (5 equiv), HOBt (0.2 M) and DIPEA (10 equiv) in DMF. Preloaded 2-chlorotrityl resins with Phe or D-Phe and Wang resins were used to synthesize peptides with free carboxylic acid in the C-terminus and Rink amide resins to obtain amidated C-terminus. Fmoc deprotection was performed using 40% piperidine/DMF for 3 min and then 20% piperidine/DMF for 14 min. In case acetylation of the *N*-terminus was required, reactions were manually carried out shaking peptides attached to the resin in a mixture of Ac2O/pyr (1:9) for five minutes three times. After

manual washings with DMF and DCM, peptides were deprotected and cleaved from the resin gently shaking in a cleavage cocktail (TFA/ TIPS/H2O 95:2.5:2.5) for 3 h. Peptides were precipitated in cold diethylether and washed three times. In case some peptides did not precipitate, TFA was removed by coevaporation with toluene using a rotary evaporator. Finally, purification was carried out by HPLC. Compound characterization can be found in the Supplementary Material.

### 2.5 In vitro assays

*In vitro* assays were manually carried out using 25 pM of protein PP1 in a buffer of 50 mM imidazole at pH 7.4 rt, 10 mM NaCl, 2 mM DTT, 1 mM $MnCl_2$ and 0.05% Triton. Assays were performed in black 96-well plates (Thermo Fisher Scientific) and all compounds were dissolved in water or mixtures of water and DMSO and then diluted in assay buffer. DiFMUP was used at a concentration of 50 μM. Fluorescence of the hydrolysis product DiFMU was measured at 25°C every 15 s during 30 min on a Tecan Infinite M1000 PRO using a 358 nm excitation wavelength and a 452 nm emission wavelength.

PP1 was first incubated for 10 min with Inhibitor-2 on ice using a concentration of Inhibitor 2 that led to 50% inhibition of PP1, which was around 10 pM. As a control, an experiment using 10% inhibition was carried out with compounds **32** and PDP3. After that, different concentrations of compounds were incubated for 20 min at room temperature to compete with Inhibitor 2 for binding to the RVxF binding site of PP1. Then, DiFMUP was added and the fluorescence was immediately measured. The initial linear part of the slopes was measured and $EC_{50}$s were determined by fitting the inhibition data with GraphPad Prism. Experiments were done in triplicates and two or more independent experiments were conducted depending on the amount of compound obtained and required for each experiment.

### 2.6 ALPHA assay

The assay buffer consisted of 50 mM TrisCl pH 7.5 rt, 150 mM NaCl, 0.05% Tween 20, 1 mM $MnCl_2$ and 0.1% BSA. 200 nM of His-PP1 and 67 nM of Biotin-PDP2[13,15] were mixed in a 384 well plate. Serial dilutions of **1** starting from 10 mM were added and incubated for 60 min at room temperature. After that, a final concentration of 5 μg/ml of streptavidin-donor and anti-His-acceptor beads were added and incubated in a final volume of 15 μl/well for 90 min at room temperature in the dark. Finally, an excitation wavelength of 680 nm was used and fluorescence at 570 nm was measured in an Envision plate reader from PerkinElmer. As a control for non-specific interactions, the same concentrations of **1** were incubated with 22 nM of GST(His-Biotin) instead of His-PP1 and Biotin-PDP2 and the assay was carried out under the same assay conditions.

### 2.7 ITC

PP1 was dialyzed in the ITC buffer consisting of 20 mM TrisCl pH 7.4 rt, 200 mM NaCl, 1 mM TCEP. The precipitated protein was removed and the rest was concentrated. The concentration, measured with Nanodrop ND-1000 spectrophotometer, was 0.72 mg/ml or 19.16 μM. In the case of Inhibitor 2, it was dialyzed in the ITC buffer and its final concentration was 0.3 mg/ml or 13.16 μM. Compound **35** was dissolved in the last dialysis

buffer used for protein sample preparation and the same buffer solution was used as the reference solution. ITC was performed at 25°C using MicroCal $ITC_{200}$ micro calorimeter (GE Health-care). The protein solution was placed in the calorimetric cell and injections of 1.8 μl of a solution of 500 μM of **35** were added into a solution of protein every 2 min. ITC data for the interactions were corrected for the dilution heat and analyzed using the MicroCal Origin™ software package.

### 2.8 Calcium release assay

HeLa Kyoto cells were maintained in DMEM low in glucose, supplemented with 10% FBS, 1% Penicillin/Streptomycin and 1% L-gluta-mine in 10 cm dishes at 37 °C with 5% $CO_2$. Cells were seeded in eight-chambered LabTeks (from VWR) with expected 80% confluency the day before imaging using an Olympus FV1200 confocal laser scanning microscope (Advanced light microscopy facility at EMBL) equipped with a 60x oil immersion objective and two scanners. For the extracellular calcium-free imaging, an LSM-DUO-Live microscope was used (Light imaging center at the University of Freiburg).

Concerning the calcium release assay to evaluate PP1 activity in intact cells, HeLa cells were incubated with 0.5 μM Fluo-4 in imaging buffer (20 mM HEPES pH 7.4 rt, 115 mM NaCl, 1.2 mM $MgCl_2$, 1.2 mM $CaCl_2$, 1.2 mM $K_2HPO_4$ and 2 g/l D-glucose) for 30 min at room temperature. For calcium-free imaging the same buffer without $CaCl_2$ containing 250 μM EGTA was used. Cells were washed with warm imaging buffer and they were excited at 488 nm and recorded at 516 nm for two minutes to confirm the absence of calcium transients. After that, compounds were added and cells were recorded for 30 min. Image processing was performed using ImageJ Software.

## 3 Results and discussion

### 3.1 High throughput and structure-based virtual screening to find PP1 binders

Initially, we attempted two often used approaches to find small molecule binders, namely *in silico* and high throughput screening (HTS). For the *in silico* screening of commercially available small molecules, 2.8 million commercially available compounds were docked against the crystal structure of PP1 bound to PDP2,[13] with PDP2 removed. The region that interacts with the sequence RVTF of the co-crystallized peptide

PDP2 was defined as the docking site. All small molecules were flexibly docked into this region. After filtering for a high docking score the docked poses of the compounds were checked for fulfilling at least two of the four pharmacophoric features, which were two hydrophobic groups, a hydrogen bond donor and a hydrogen bond acceptor (Supp. Fig. 1). These were identified to be important for binding after visual inspection of crystal structures of PP1 with RIPPOs binding to the RVxF binding site. 58 compounds were finally prioritized and purchased for *in vitro* testing. For the HTS, a library of 79,000 compounds available at the Chemical Biology Core Facility at EMBL was screened. As for the development of PDP-*Nal*,[20] dephosphorylation of the unnatural substrate 6,8-difluoro-4-methylumbelliferyl phosphate (DiFMUP) was measured as read-out of the biochemical screen. The assay was optimized to achieve around 80% inhibition of PP1 by its native

inhibitory protein inhibitor-2 (I2) without compound treatment, leading to a linear increase in fluorescence over 3 h. This made the assay suitable to find compounds disrupting the interaction of the inactive PP1:I2 holoenzyme, leading to de-inhibition of PP1 by releasing the catalytic subunit as measured by an increase in the fluorescence signal. From the screen of 79,000 compounds, 58 compounds inducing over 40% of PP1 activity were selected and purchased from the suppliers. Together with the compounds from the virtual screen, they were tested to confirm their activity in the screening assay in dose-response and in parallel for specificity of their effect on PP1 phosphatase activity in a counter assay without PP1:I2 in the reagent mix. A PDP served as internal positive control standard on each assay plate. The activity in the PP1 screening assay could be confirmed for only 13 of the 58 re-ordered compounds from the initial HTS. All these compounds showed mostly strong auto-fluorescence and their effect on the increase of fluorescence over time was not specific for the phosphatase-activity of PP1:I2, as they all had a similar effect in the counter assay without PP1:I2. Most probably these compounds aggregate slowly in aqueous buffer causing an increase of their intrinsic fluorescence. Only 3 of the 58 compounds from the docking approach showed a moderate activity in the PP1:I2-assay, but all were fluorescent and had a similar activity in the counter assay without PP1:I2. In summary, using the kinetic measurement we could overcome most well-known problems of assays based on short-wavelength fluorescence substrates and identify putative small-molecule antagonists in the primary screen. The methodology was sound in that the PDP produced consistent results. However, none of the small molecule hit compounds from the HTS or virtual screen could be confirmed as PP1/I2-specific. This outcome showed the difficulty to target protein-protein interactions with small molecules and encouraged us to optimize and shorten the peptide-based modulators.

### 3.2 Development of short peptidomimetics as PP1 binders

As a starting point for the development of these peptidic compounds, a short tetrapeptide with the sequence RVTF (**1**) was prepared because it is the part of PDPs that binds to the RVxF binding site of PP1.[13] The ability of **1** to disrupt the interaction between PP1 and the I2 was tested *in vitro* giving an $EC_{50}$ of 234 ± 48.6 μM (Table 1). In order to validate that **1** binds to the same site as the PDPs, an Amplified Luminescent Proximity Homogeneous Assay (ALPHA), where **1** competed with a PDP for binding to the RVxF binding site of PP1, was performed, resulting in an $IC_{50}$ of 124 μM. After these encouraging results, chemically similar proteinogenic amino acids were replaced one by one in the sequence of RVTF (**1**). The results displayed in Table 1 showed that arginine and valine were the most favorable amino acids in the first and second position, respectively. Regarding the “x” position, it was discovered that a hydrogen-bond donating group was required, achieving the highest potency in the presence of histidine (**9**). Interestingly, histidine is also found in the equivalent “x” position of several RIPPOs such as I2[22] and spinophilin,[23] where the imidazole group binds to Thr288 in PP1. This additional interaction could be responsible for the higher potency of **9**. Concerning the fourth position, peptides were more active with phenylalanine but also tolerated tryptophan (**18**).

With the purpose of understanding the relevance of the stereochemistry of the amino acid side chains and to increase the stability of the peptides,[24] L-amino acids were exchanged

with D-amino acids one by one (**19**-**22**) and two random combinations were also tested (**23** and **24**). However, none of the resulting compounds were active (Table 1), showing that L-amino acid stereochemistry was required for potency. Moreover, the reverse peptide (**25**) was also inactive. The retroinverse peptide, which is probably the most related isosteric substitution of the peptide bond[25] while being less susceptible to proteolysis due to the presence of non-proteinogenic amino acids,[26] was evaluated with both threonine (**26**) and histidine (**27**) in the equivalent "x" position. None of them were active, indicating that the overall stereochemistry and conformation did not allow changes without losing potency.

Additionally, both termini were modified trying to mimic native proteins and increasing their proteolytic stability. Acetylation of the *N*-terminus (**28**) produced an inactive peptide probably due to observed gel formation and insolubility issues. However, amidation of the *C*-ter-minus (**29**) increased the potency. The combination of both termini modifications (**30**) again slightly increased the potency, showing that *C*-terminal amidation was beneficial and *N*-acetylation did not abolish binding to PP1 (Table 1).

With the aim of increasing the potency, peptides were *N*-terminally extended with arginine or lysine because many RIPPOs contain a highly flexible polybasic sequence connected to the *N*-terminus of the RVxF sequence.[27] As expected, pentapeptides RRVHF (**31**) and KRVHF (**32**) showed an increase in potency (Table 1). KRVHF (**32**) was around 30-fold less potent than the parent compound PDP3 (8 μM vs. 233 nM, respectively), which is quite remarkable given the difference in length of 18 amino acids missing in KRVHF (Supp. Fig. 2A and B, respectively). *N*-Acetylation, Ac-KRVHF (**33**) and together with *C*-amidation, Ac-KRVHF-$NH_2$ (**34**), did not increase the potency. As observed with the potency increase of **29**, *C*-terminal amidation of **32**, KRVHF-$NH_2$ (**35**), led to the most active pentapeptide with an EC50 of 609 ± 38.6 nM (Supp. Fig. 2C). Of note, a previously reported 6mer peptide RKIQFT gave at a comparable starting inhibition of PP1 by I2 of 50% an EC50 of 54 μM,[15] demonstrating the value of sequence optimization. Taken together, after several rounds of rational sequence optimization of short peptides starting with RVTF (**1**), it was possible to increase their potency from 3-digit micromolar to sub-micromolar concentrations, which is quite remarkable considering the difficulties in targeting this site.[28]

Next, in order to increase the stability of the peptides peptidomimetics based on the most active peptide **35** but containing non-proteinogenic amino acids and modifications such as *N*-methyl, beta, homo, beta-homo and non-natural side chain amino acids (**36**-**50**) were rationally designed and tested *in vitro* (Table 1). Although the most active compound (**35**) contained natural lysine, this position admitted more variability than other positions without a dramatic impact on the activity. Regarding substitutions in the position of arginine, replacement with homo-arginine (**43**) led to one of the most active peptidomimetics *in vitro* (Supp. Fig. 2D). Valine was replaced with L-cyclopropylglycine (Cpg) (**46**) restricting the conformation and angles of the side chain, but the potency decreased. In the position of phenylalanine, the importance of the aromaticity and planarity of the phenyl group was confirmed as well as the decrease in efficacy in the presence of naphtylalanine (NaI), where unlike other compounds, **48** and **49** only reached around 80% of PP1 activity (Supp. Fig. 2E

and F, respectively), which suggested that the hydrophobic pocket is not big enough to fit the two fused rings. Still, peptide **35** remained to be the most potent compound.

We then aimed at showing that **35** bound specifically to PP1 and not to I2 by Isothermal Titration Calorimetry (ITC). While compound **35** bound to PP1 in a molar ratio of 1:1 with a dissociation constant of 2.1 ± 0.4 μM (ΔH = -6580 ± 74 cal/mol and ΔS = 3.94 cal/mol/deg) (Fig. 2A), no interaction was detected between **35** and I2 (Fig. 2B), confirming that **35** specifically bound to PP1 in this assay.

### 3.3 Evaluation of the cellular activity of the peptidomimetic PP1 binders

Next, we aimed at testing whether the most active compounds would show activity in intact cells. As previously reported, histone H3 phosphorylated on threonine 3 (H3pT3) during mitosis is a substrate of PP1, and PDP treatment promoted its dephosphorylation during mitotic arrest.[13,20] Therefore, we screened a range of the most potent pentapeptides (**33**-**41**, **43**, **45**, **46**) for their ability to trigger H3pT3 dephosphorylation in U2OS cells at a concentration of 100 μM using the reported method.[13] Unfortunately, none of the peptides were reproducibly active in this assay (data not shown). Since this assay requires longer incubation times (at least 30 min) and mitotic arrest[13,20] which could have an effect on the stability of the peptides, we then aimed at testing their activity in an assay with a very short incubation time. PP1 is involved in intracellular calcium release processes. Upon disruption of the interaction of PP1 with RIPPOs using PDPs, the active free catalytic subunit of PP1 induces calcium oscillations in HeLa cells.[10] With the objective of evaluating whether the developed compounds could trigger calcium sparking, intact HeLa cells were incubated with Fluo-4, a fluorescent $Ca^{2+}$-indicator dye,[29] and compounds were added to measure calcium release by fluorescence microscopy. After both negative (buffer) and positive (PDP3) control experiments were carried out (Supp. Fig. 3A,B), compounds with an *in vitro* $EC_{50}$ < 5 μM were tested in living cells. The most active compound *in vitro*, **35**, was tested at different concentrations but did not produce calcium spikes even at 10 mM (Fig. 3A). Peptidomimetics **34**, **36** and **37** were also inactive, but compounds **39**, **41**, **45** and **46** appeared slightly active with a few cells responding (Supp. Fig. 3C-I). Peptidomimetic **43** triggered the strongest response in a concentration-dependent manner (Fig. 3B,C). However, the cellular response of releasing calcium required high peptide concentrations, and did not correlate well with the $EC_{50}$s and with the presence of unnatural amino acids, which would stabilize peptides against degradation. Therefore, we asked whether the calcium originates from the inside of the cell, as is the case for the longer PDPs,[10] or if the calcium spikes depend on external calcium, which would for example occur if the peptide treatment led to a disruption in the plasma membrane and enabled external calcium to enter the cell. When we repeated the treatment of **43** in $Ca^{2+}$-free medium in the presence of ethylene glycol tetraacetic acid (EGTA, Fig. 3D) to chelate extracellular $Ca^{2+}$, we did not observe any $Ca^{2+}$ spiking anymore, suggesting that the cellular response is not PP1-dependent, and that these peptides did not act in the same manner as PDPs.[10]

## 4 Conclusions

In summary, to approach our aim to find a pharmacophore we have successfully set up a structure-based virtual and a high throughput screen. Unfortunately, no hits resulted from these screens, which shows how difficult it is to target this phosphatase. We then carried out a rational structure-activity relationship study of short peptides and peptidomimetics binding to the RVxF binding site of PP1, revealing information about the functional groups required for binding to the RVxF binding site. After several rounds of optimization, we were able to optimize a pentapeptide with sub-micromolar activity in disrupting the interaction between PP1 and Inhibitor-2 *in vitro*. As other short peptides before,[15] these peptides were not active in cells. Adding a poly-arginine tail could help to enhance cell penetration and with this in-cell activity,[15] however, it would defeat the purpose of reducing the peptide size and offer no advantage over the optimized PDP-*Nal*.[20] Future efforts will have to focus on strategies morphing the peptidomimetic pentapeptides into more drug-like molecules. Considering the biological relevance of PP1 in health and disease and the difficulties in targeting this allosteric site, as well as the PDP's use for phosphatase-recruiting (or targeting) chimeras (PhoRCs[18] or PhosTACs[17]), our results form an important basis for optimizing current strategies to study and target PP1.

## Supplementary Material

Refer to Web version on PubMed Central for supplementary material.

## Acknowledgements

We thank Vladimir Rybin, EMBL, for his support with the ITC measurements. We thank the ALMF at EMBL and the LIC at the University of Freiburg for their imaging support. M.K. acknowledges a starting grant (#336567) and a consolidator grant (#865119) from the European Research Council (ERC).

## References

1. Peti W, Nairn AC, Page R. Folding of intrinsically disordered protein phosphatase 1 regulatory proteins. Curr Phys Chem. 2012; 2: 107–114. DOI: 10.2174/1877946811202010107 [PubMed: 22866172]
2. Li X, Wilmanns M, Thornton J, Köhn M. Elucidating human phosphatase-substrate networks. Sci Signal. 2013; 6 rs10 doi: 10.1126/scisignal.2003203 [PubMed: 23674824]
3. Virshup DM, Shenolikar S. From promiscuity to precision: protein phosphatases get a makeover. Mol Cell. 2009; 33: 537–545. DOI: 10.1016/j.molcel.2009.02.015 [PubMed: 19285938]
4. Bollen M, Peti W, Ragusa MJ, Beullens M. The extended PP1 toolkit: designed to create specificity. Trends Biochem Sci. 2010; 35: 450–458. DOI: 10.1016/j.tibs.2010.03.002 [PubMed: 20399103]
5. Kohn M. Turn and face the strange: a new view on phosphatases. ACS Cent Sci. 2020; 6: 467–477. DOI: 10.1021/acscentsci.9b00909 [PubMed: 32341996]
6. Heroes E, Lesage B, Görnemann J, Beullens M, Van Meervelt L, Bollen M. The PP1 binding code: a molecular-lego strategy that governs specificity. FEBS J. 2013; 280: 584–595. DOI: 10.1111/j.1742-4658.2012.08547.x [PubMed: 22360570]
7. Bollen M, Gerlich DW, Lesage B. Mitotic phosphatases: from entry guards to exit guides. Trends Cell Biol. 2009; 19: 531–541. DOI: 10.1016/j.tcb.2009.06.005 [PubMed: 19734049]
8. Aoyama H, Ikeda Y, Miyazaki Y, et al. Isoform-specific roles of protein phosphatase 1 catalytic subunits in sarcoplasmic reticulum-mediated Ca(2+) cycling. Cardiovasc Res. 2011; 89: 79–88. DOI: 10.1093/cvr/cvq252 [PubMed: 20675715]

9. Hafver TL, Hodne K, Wanichawan P, et al. J Biol Chem. 2016; 291: 4561–4579. DOI: 10.1074/jbc.M115.677898 [PubMed: 26668322]
10. Reither G, Chatterjee J, Beullens M, Bollen M, Schultz C, Köhn M. Chemical activators of protein phosphatase-1 induce calcium release inside intact cells. Chem Biol. 2013; 20: 1179–1186. DOI: 10.1016/j.chembiol.2013.07.008 [PubMed: 23972940]
11. Chiang DY, Li N, Wang Q, et al. Impaired local regulation of ryanodine receptor type 2 by protein phosphatase 1 promotes atrial fibrillation. 2014; 103: 178–87. DOI: 10.1093/cvr/cvu123
12. Fischer TH, Eiringhaus J, Dybkova N, et al. Activation of protein phosphatase 1 by a selective phosphatase disrupting peptide reduces sarcoplasmic reticulum Ca2+ leak in human heart failure. Eur J Heart Fail. 2018; 20: 1673–1685. DOI: 10.1002/ejhf.1297 [PubMed: 30191648]
13. Chatterjee J, Beullens M, Sukackaite R, et al. Development of a peptide that selectively activates protein phosphatase-1 in living cells. Angew Chem Int Ed. 2012; 51: 10054–10059. DOI: 10.1002/anie.201204308
14. Kwon YG, Huang HB, Desdouits F, Girault JA, Greengard P, Nairn AC. Characterization of the interaction between DARPP-32 and protein phosphatase 1 (PP-1): DARPP-32 peptides antagonize the interaction of PP-1 with binding proteins. Proc Natl Acad Sci U S A. 1997; 94: 3536–3541. DOI: 10.1073/pnas.94.8.3536 [PubMed: 9108011]
15. Sotoud H, Borgmeyer U, Schulze C, El-Armouche A, Eschenhagen T. Development of phosphatase inhibitor-1 peptides acting as indirect activators of phosphatase 1. Naunyn Schmiedebergs Arch Pharmacol. 2015; 388: 283–293. DOI: 10.1007/s00210-014-1065-2 [PubMed: 25416155]
16. Tappan E, Chamberlin AR. Activation of protein phosphatase 1 by a small molecule designed to bind to the enzyme's regulatory site. Chem Biol. 2008; 15: 167–174. DOI: 10.1016/j.chembiol.2008.01.005 [PubMed: 18291321]
17. Chen PH, Hu Z, An E, et al. Modulation of phosphoprotein activity by phosphorylation targeting chimeras (PhosTACs). ACS Chem Biol. 2021; 16: 2808–2815. DOI: 10.1021/acschembio.1c00693 [PubMed: 34780684]
18. Yamazoe S, Tom J, Fu Y, et al. Heterobifunctional molecules induce dephosphorylation of kinases-a proof of concept study. J Med Chem. 2020; 63: 2807–2813. DOI: 10.1021/acs.jmedchem.9b01167 [PubMed: 31874036]
19. Sotoud H, Gribbon P, Ellinger B, et al. Development of a colorimetric and a fluorescence phosphatase-inhibitor assay suitable for drug discovery approaches. J Biomol Screen. 2013; 18: 899–909. DOI: 10.1177/1087057113486000 [PubMed: 23606651]
20. Wang Y, Hoermann B, Pavic K, Trebacz M, Rios P, Köhn M. Interrogating PP1 activity in the MAPK pathway with optimized PP1-Disrupting Peptides. ChemBioChem. 2019; 20: 66–71. DOI: 10.1002/cbic.201800541 [PubMed: 30338897]
21. Wishart DS, Bigam CG, Yao J, et al. 1H, 13C and 15N chemical shift referencing in biomolecular NMR. J Biomol NMR. 1995; 6: 135–140. DOI: 10.1007/BF00211777 [PubMed: 8589602]
22. Yang J, Hurley TD, DePaoli-Roach AA. Interaction of inhibitor-2 with the catalytic subunit of type 1 protein phosphatase. Identification of a sequence analogous to the consensus type 1 protein phosphatase-binding motif. J Biol Chem. 2000; 275: 22635–22644. DOI: 10.1074/jbc.M003082200 [PubMed: 10807923]
23. Ragusa MJ, Dancheck B, Critton DA, Nairn AC, Page R, Peti W. Spinophilin directs protein phosphatase 1 specificity by blocking substrate binding sites. Nat Struct Mol Biol. 2010; 17: 459–464. DOI: 10.1038/nsmb.1786 [PubMed: 20305656]
24. Tugyi R, Uray K, Iván D, Fellinger E, Perkins A, Hudecz F. Partial D-amino acid substitution: improved enzymatic stability and preserved Ab recognition of a MUC2 epitope peptide. Proc Natl Acad Sci USA. 2005; 102: 413–418. DOI: 10.1073/pnas.0407677102 [PubMed: 15630090]
25. Chorev M, Goodman M. A dozen years of retro-inverso peptidomimetics. Acc Chem Res. 26: 1993; 266–73. DOI: 10.1021/ar00029a007
26. Chorev M, Goodman M. Recent developments in retro peptides and proteins - an ongoing topochemical exploration. Trends Biotechnol. 1995; 13: 438–445. DOI: 10.1016/S0167-7799(00)88999-4 [PubMed: 7546569]

27. O'Connell N, Nichols SR, Heroes E, et al. The molecular basis for substrate specificity of the nuclear NIPP1:PP1 holoenzyme. Structure. 2012; 20: 1746–1756. DOI: 10.1016/j.str.2012.08.003 [PubMed: 22940584]

28. Chatterjee J, Köhn M. Targeting the untargetable: recent advances in the selective chemical modulation of protein phosphatase-1 activity. Curr Opin Chem Biol. 2013; 17: 361–368. DOI: 10.1016/j.cbpa.2013.04.008 [PubMed: 23647984]

29. Geek KR, Brown KA, Chen WN, Bishop-Stewart J, Gray D, Johnson I. Chemical and physiological characterization of fluo-4 Ca(2+)-indicator dyes. Cell Calcium. 2000; 27: 97–106. DOI: 10.1054/ceca.1999.0095 [PubMed: 10756976]



Europe PMC Funders Author Manuscripts

Europe PMC Funders Author Manuscripts

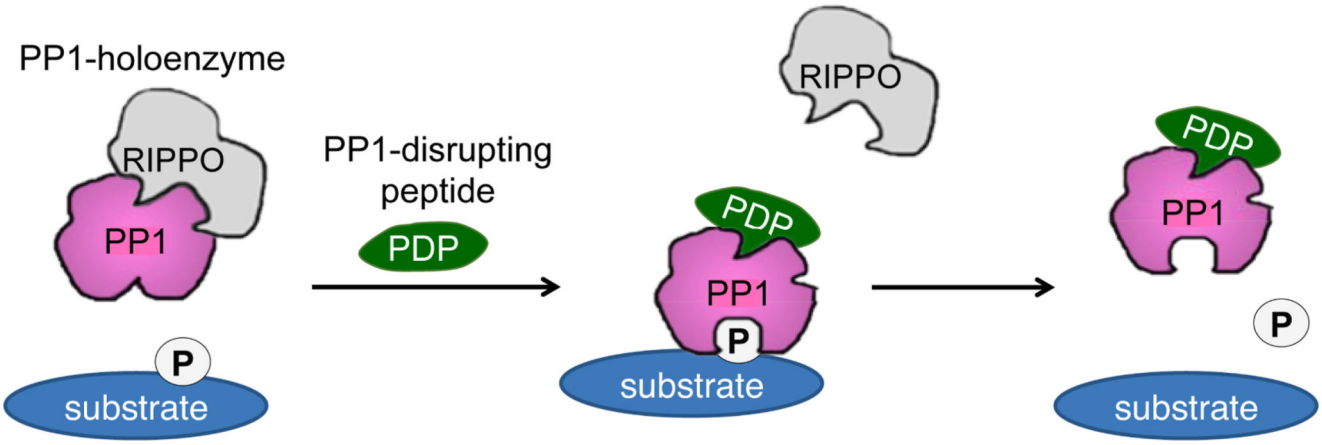


**Fig. 1. Mechanism of action of PDPs.**

PP1 is bound to regulatory proteins (RIPPOs) in cells. These specify its interactions and activity. Through binding to the allosteric RVxF-binding site, PDPs disrupt these holoenzymes and release PP1 catalytic unit, which can dephosphorylate nearby substrates. Inhibitory RIPPOs, in particular Inhibitor-2 (I2), bind to the active site and the RVxF-binding site (Protein Data Bank PDB code 2O8A and 2O8G), thereby blocking the activity. Replacement of I2 with a PDP therefore leads to de-inhibition by de-blocking the active site.

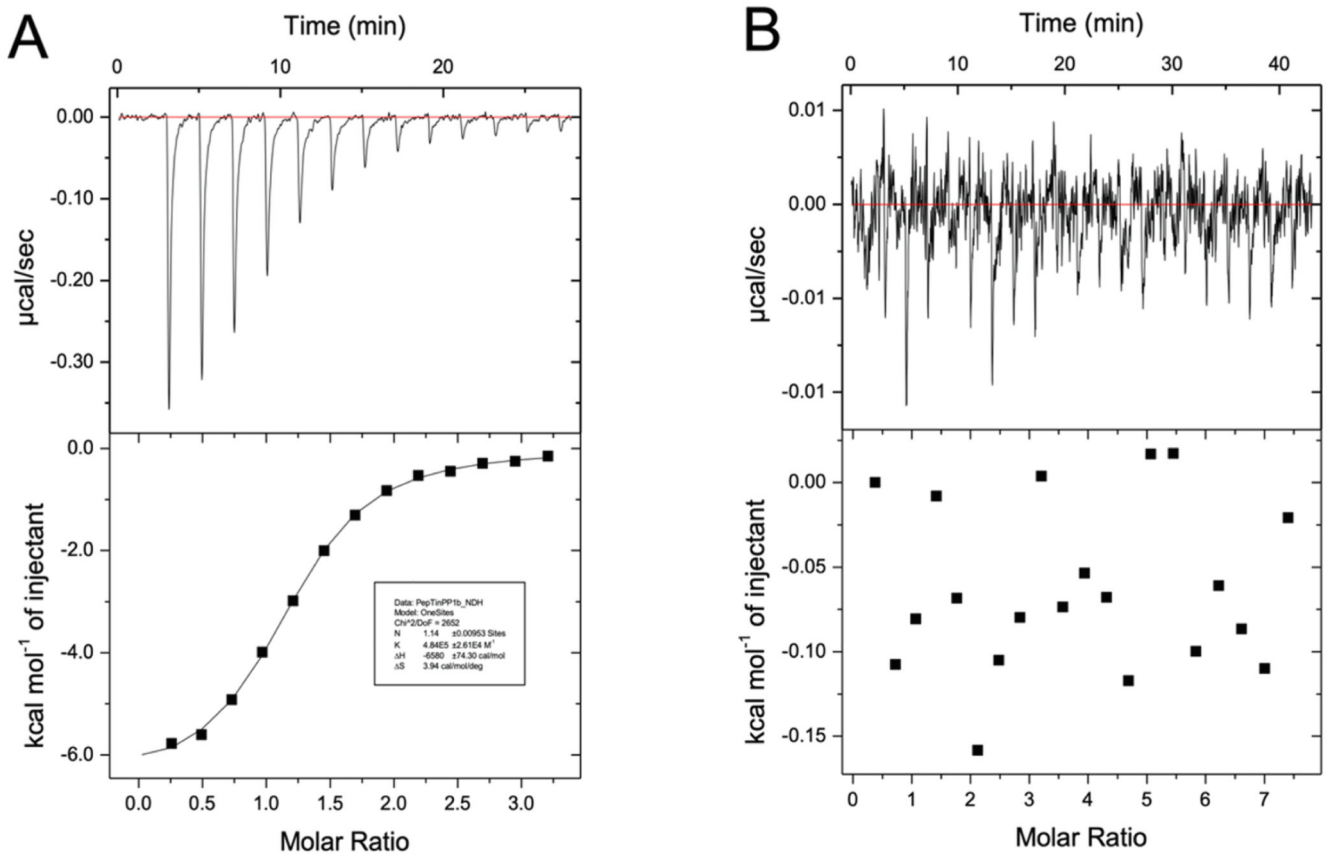


**Fig. 2.**

ITC measurement at 25 °C with VP-ITC Microcal calorimeter (Microcal, Northhampton, MA, USA). Raw data (upper part) and processed data (lower part). ITC measurements were carried out in a buffer of 20 mM TrisCl at pH 7.4 rt, 200 mM NaCl, 1 mM TCEP using 500 µM of **35** and (**A**) 0.72 mg/ml of PP1 or (**B**) 0.3 mg/ ml of Inhibitor 2.




Europe PMC Funders Author Manuscripts

Europe PMC Funders Author Manuscripts

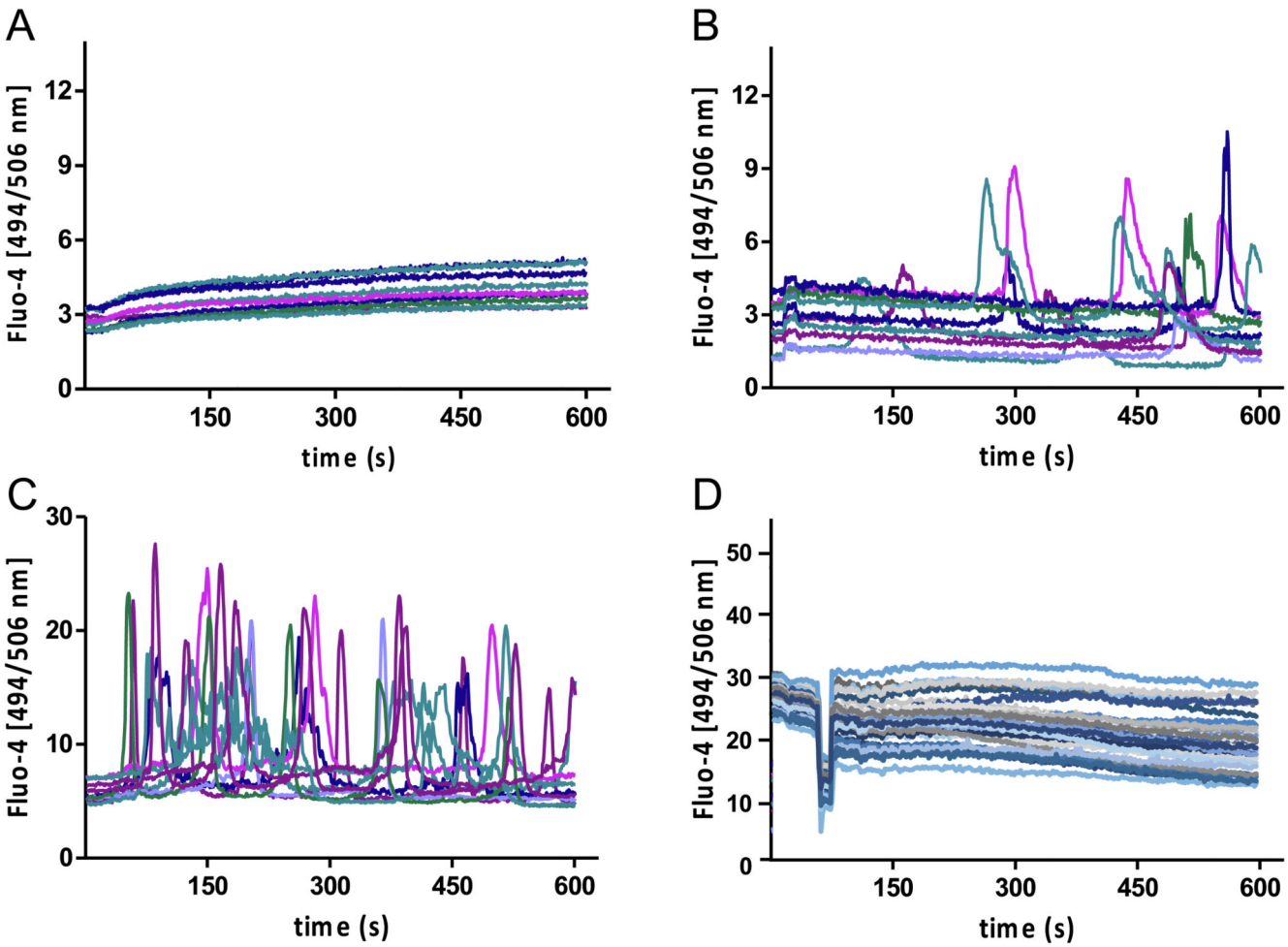


**Fig. 3.**

Induction of calcium transient release in HeLa Cells measured by fluorescent $Ca^{2+}$-indicator dye Fluo-4 imaging. Representative traces of ten cells are plotted. In all cases, compounds were added 10 s after starting the recording. (**A**) 10 mM **35** (total n = 80 cells, 0% responder). (**B**) 100 μM **43** (total n = 136 cells, 35% responder). (**C**) 500 μM **43** (total n = 53 cells, 47% responder). (**D**) Incubation of HeLa cells in imaging buffer containing no $Ca^{2+}$ and 250 mM EGTA with 500 μM **43** (total n = 30 cells, 0% responder, higher background due to different microscope used).

## Table 1

$EC_{50}$ (μM) of the disruption of the interaction between PP1 and Inhibitor 2 with compounds, where D-amino acids are indicated with “d” before the one letter code and amino acids rationally changed from the sequence of RVTF (**1**) are in bold. $EC_{50}$s (μM) of pentapeptides **31-50**, where amino acids changed from KRVHF-$NH_2$ (**35**) are in bold. $EC_{50}$s where measured starting at 50% inhibition of PP1 with I2 and using DiFMUP as a substrate (see Methods).

| Compound | Sequence | EC50 (μM) |
|---|---|---|
| **1** | RVTF | 234 ± 48.6 |
| **2** | **K**VTF | > 500 |
| **3** | R**I**TF | Slightly active at 500 μM |
| **4** | R**L**TF | Slightly active at 500 μM |
| **5** | RV**S**F | > 500 |
| **6** | RV**G**F | Slightly active at 500 μM |
| **7** | RV**V**F | Slightly active at 500 μM |
| **8** | RV**K**F | 249 ± 51.0 |
| 9 | RV**H**F | 69.7 ± 18.1 |
| **10** | RV**N**F | 220 ± 53.8 |
| **11** | RV**Q**F | 224 ± 82.1 |
| **12** | RV**D**F | > 500 |
| 13 | RV**E**F | Slightly active at 500 μM |
| **14** | RV**F**F | > 500 |
| **15** | RV**Y**F | Slightly active a 500 μM |
| **16** | RV**W**F | 104 ± 39.6 |
| 17 | RVT**Y** | > 500 |
| **18** | RVT**W** | 256 ± 59.8 |
| **19** | d**R**VTF | > 500 |
| **20** | Rd**V**TF | > 500 |
| **21** | RV**dT**F | > 500 |
| **22** | RVT**dF** | > 500 |
| **23** | **dRdVdT**F | > 500 |
| **24** | **dR**VT**dF** | > 500 |
| 25 | **FTVR** | > 500 |
| **26** | **dFdTdVdR** | > 500 |
| **27** | **dFdHdVdR** | Slightly active at 500 μM |
| **28** | **Ac**-RVTF | > 500 |
| **29** | RVTF-**$NH_2$** | 101 ± 11.1 |
| **30** | Ac-RVTF-**$NH_2$** | 85.7 ± 1.6 |
| **31** | RRVHF | 2.7 ± 0.6 |
| **32** | KRVHF | 1.5 ± 0.6 |
| **33** | Ac-KRVHF | 3.2 ± 0.5 |
| **34** | Ac-KRVHF-$NH_2$ | 1.7 ± 0.1 |

Europe PMC Funders Author Manuscripts

| Compound | Sequence | EC50 (μM) |
|---|---|---|
| **35** | KRVHF-$NH_2$ | 0.6 ± 0.04 |
| **36** | **dK**RVHF-$NH_2$ | 2.6 ± 0.4 |
| **37** | (**β-K**)-RVHF-$NH_2$ | 2.9 ± 0.1 |
| **38** | (β-homo-K)-RVHF-$NH_2$ | 9.8 ± 0.2 |
| **39** | **Orn**-RVHF-$NH_2$ | 4.1 ± 0.1 |
| **40** | (**homo-R**)-RVHF-$NH_2$ | 6.6 ± 0.2 |
| **41** | (**β-homo-R**)-RVHF-$NH_2$ | 3.2 ± 0.2 |
| **42** | K**H**VHF-$NH_2$ | 24.6 ± 2.1 |
| **43** | K-(**homo-R**)-VHF-$NH_2$ | 1.7 ± 0.2 |
| **44** | K-(**β-homo-R**)-VHF-$NH_2$ | 204 ± 1.9 |
| **45** | K-(***N*-Me-R**)-VHF-$NH_2$ | 4.7 ± 0.3 |
| **46** | KR-**Cpg**-HF-$NH_2$ | 2.1 ± 0.1 |
| **47** | KRVH-**Cha**-$NH_2$ | 52.5 ± 1.8 |
| **48** | KRVH-(**1-NaI**)-$NH_2$ | 2.5 ± 0.2 |
| **49** | KRVH-(**2-NaI**)-$NH_2$ | 1.5 ± 0.4 |
| **50** | KRVH-(***N*-Me-F**)-$NH_2$ | 23.5 ± 0.7 |